Contribution from the Department of Chemistry,
The University of Western Ontario, London, Ontario N6A 5B7, Canada

Complexes of Hybrid Ligands. Synthesis of a Fluoro-Alcohol Diarylphosphino Ligand and Its Complexes with Pt^{2+}, Pd^{2+}, Ni^{2+}, Co^{2+}, Cu^{+}, and Rh^{3+}: Crystal and Molecular Structure of a Trans Square-Planar Ni^{2+} Complex with Two Bidentate Ligands Showing Cis-Trans Isomerism in Solution[1]

RENÉ T. BOERÉ, CRAIG D. MONTGOMERY, NICHOLAS C. PAYNE,* and CHRISTOPHER J. WILLIS*

Received February 13, 1985

The first example of a fluorinated alcohol containing a tertiary phosphino function, $PPh_2CH_2C(CF_3)_2OH$ (HL^1), has been synthesized. In the ionized form, this compound acts as a uninegative, bidentate, chelating, hybrid ligand, capable of forming stable complexes with both hard and soft transition-metal ions. We have made $Pt(L^1)_2$, $Pd(L^1)_2$, $Ni(L^1)_2$, $Co(L^1)_2$, $Cu(L^1)(PPh_3)_2$, and $K[RhCl_2(L^1)_2]$. NMR data show that $Pt(L^1)_2$ and $Pd(L^1)_2$ are cis square-planar compounds in solution. In solution, $Ni(L^1)_2$ is a mixture of cis and trans isomers, and values of ΔH, ΔG, and ΔS for their interconversion in different solvents are derived from variable-temperature NMR spectra. The CH_2 ^1H and CF_3 ^{19}F NMR signals in the ligand appear as pseudotriplets in both cis *and* trans isomers of $Ni(L^1)_2$, through coupling to ^{31}P nuclei in the two ligand molecules. This "virtual coupling" is the result of large $^2J(P,P')$ values in both isomers. A complete determination of the crystal and molecular structure has been made for $Ni(L^1)_2$, $C_{32}H_{24}F_{12}NiO_2P_2$. Crystals are orthorhombic, space group $P2_12_12_1$, with a = 18.145 (2) Å, b = 33.269 (3) Å, c = 10.945 (1) Å, V = 6607 (2) Å^3, and Z = 8. Least-squares refinement on F of 407 variables using 5922 observations converged at a conventional agreement factor R = 0.072. The complex is trans square planar in configuration, but there are two significantly different molecular conformations present. In one of these, there are close approaches to nickel from the CF_3 groups of the ligand; this interaction distorts the ligand field around the metal and produces a difference in color between the solid and the solution of this complex.

Introduction

We have earlier described the synthesis and application of hybrid, bidentate ligands in which the hard fluorinated alkoxy function is combined with a soft thioether ligand, giving on ionization $R-S-CH_2-C(CF_3)_2-O^-$, which chelates to Pd^{2+} and Pt^{2+}.[2] With fluorinated alkoxides, a second donor site in the ligand is usually necessary to stabilize, by chelation, the bond to $RC(CF_3)_2O^-$, and complexes derived from monodentate ligands such as $(CF_3)_3CO^-$ are confined to oxophilic ions such as uranium(V)[3] or oxomolybdenum(VI).[4]

A hybrid ligand of this type would be more useful if it contained a combination of the fluoro alcohol with an alkyl- or arylphosphino group, which would bond more strongly, and to a wider variety of metals, than the thioether function. Previous work on hybrid ligands has led to the synthesis of a variety of complexes containing a soft phosphino group and a hard oxygen donor, and examples are known where the latter function is ether,[5] ester,[6] carboxylate,[7] ketone,[8] or phenoxide.[9] Such ligands may function either by chelation,[7,9] by unidentate coordination through phosphorus,[10] or by bridging between homo- or heteronuclear metal centers.[11]

We have therefore synthesized the fluorinated alcohol $Ph_2P-CH_2-C(CF_3)_2OH$ and studied its interaction (in the ionized form) with transition-metal ions. We expected the new ligand to form complexes in which the soft phosphine donor stabilizes the bond between a heavy transition-metal ion and the hard alkoxy function and also to coordinate to first-row transition-metal ions of hard or intermediate character, for which phosphino complexes are well-known.

In this paper, we demonstrate the applicability of this ligand to ions of differing character by the preparation of neutral bis complexes $M[Ph_2PCH_2C(CF_3)_2O]_2$, where M = Co^{2+}, Ni^{2+}, Pd^{2+}, or Pt^{2+}, together with the Cu^+ complex $Cu(PPh_3)_2[Ph_2PCH_2C(CF_3)_2O]$ and the anionic Rh^{3+} complex $[RhCl_2[Ph_2PCH_2C(CF_3)_2O]_2]^-$. For the nickel(II) complex, a structural determination shows the ligands to be trans disposed in the solid state, while NMR studies reveal a solvent- and temperature-dependent equilibrium between cis and trans isomers in solution. A significant color change between solid and solution may be accounted for in terms of intramolecular interactions between the metal ion and CF_3 groups on the chelating ligands in the solid.

Experimental Section

General Information. Microanalysis was performed by Guelph Analytical Laboratories, Guelph, Ontario, Canada; analytical data are in Table I. Infrared spectra were recorded on a Beckman 4250 spectrometer, mass spectra on a Varian MAT 311A instrument, and NMR spectra on a Varian XL-100 spectrometer at 100.1 MHz for ^1H, 94.1 MHz for ^{19}F, and 40.5 MHz for ^{31}P; all ^{31}P spectra were proton-decoupled. Chemical shifts are reported relative to Me_4Si, $CFCl_3$, or $(MeO)_3PO$ (external), respectively; positive shifts are to low field. Variable-temperature NMR spectra were recorded over the range −15 to +75 °C. Temperature settings of the spectrometer were checked with a Doric Trendicator 400 Type T digital thermometer calibrated to ±0.5 °C at the ice point. NMR data are in Table V.

Volatile compounds were manipulated on a conventional vacuum line. Glass apparatus and solvents were rigorously dried before use for ligand preparation. Air-sensitive materials were transferred by using serum caps and syringes. *n*-Butyllithium, *N,N,N',N'*-tetramethylethylenediamine (TMED), and methyldiphenylphosphine were commercial samples (Aldrich).

Ligand Synthesis. Lithiation of methyldiphenylphosphine was carried out according to Peterson's procedure.[12] A 1.6 M solution of *n*-butyllithium in hexane (44 mL, 70 mmol) was transferred by syringe under argon into a dry round-bottom flask, followed by TMED (10.6 mL, 70 mmol) and $PMePh_2$ (14.5 mL, 70 mmol). After the mixture was stirred for 20 min, a bright yellow precipitate (Ph_2PCH_2Li·TMED) had formed, which was dissolved by the addition of dry THF (30 mL). The solution was cooled to −78 °C and hexafluoroacetone (12.0 g, 72 mmol; Matheson) passed in in a stream of dry nitrogen. The reaction mixture was then poured into concentrated HCl (100 mL) at 0 °C and extracted with Et_2O (3 × 150 mL). After drying (Na_2SO_4), the ether was removed by rotary evaporation and the remaining oil distilled under vacuum to give 2-(di-

(1) Presented in part at the XXIIIrd International Conference on Coordination Chemistry, Boulder, CO, Aug 1984.
(2) Boerē, R. T.; Willis, C. J. "Abstracts of Papers", 10th International Symposium on Fluorine Chemistry, Vancouver, BC, 1982; *J. Fluorine Chem.* **1982**, *21*, 18.
(3) Eller, P. G.; Vergamini, P. J. *Inorg. Chem.* **1983**, *22*, 3184.
(4) Johnson, D. A.; Taylor, J. C.; Waugh, A. B. *J. Inorg. Nucl. Chem.* **1980**, *42*, 1271.
(5) (a) Jeffrey, J. C.; Rauchfüss, T. B. *Inorg. Chem.* **1979**, *18*, 2658. (b) Anderson, G. K.; Kumar, R. *Inorg. Chem.* **1984**, *23*, 4064.
(6) Braunstein, P.; Matt, D.; Dusausay, Y. *Inorg. Chem.* **1983**, *22*, 2043.
(7) (a) Podlahová, J.; Kratochvil, B.; Langer, V. *Inorg. Chem.* **1981**, *20*, 2160. (b) Civis, S.; Podlahová, J.; Loub, J. *Acta Crystallogr., Sect. B: Struct. Crystallogr. Cryst. Chem.* **1980**, *B36*, 1395.
(8) Empsall, H. D.; Johnson, S.; Shaw, B. L. *J. Chem. Soc., Dalton Trans.* **1980**, 302.
(9) O'Flynn, K. H. P.; McDonald, W. S. *Acta Crystallogr., Sect. B: Struct. Crystallogr. Cryst. Chem.* **1977**, *B33*, 194.
(10) Braunstein, P.; Matt, D.; Dusausay, Y.; Fischer, J.; Mitschler, A.; Ricard, L. *J. Am. Chem. Soc.* **1981**, *103*, 5115.
(11) Farr, J. P.; Olmstead, M. M.; Balch, A. L. *J. Am. Chem. Soc.* **1980**, *102*, 6654.
(12) Peterson, D. J. *J. Organomet. Chem.* **1967**, *8*, 199.

0020-1669/85/1324-3680$01.50/0

Table I. Analytical Data

no.	compd	formula	% carbon calcd	% carbon found	% hydrogen calcd	% hydrogen found	% phosphorus calcd	% phosphorus found
2	$Pt(L^1)_2$	$C_{32}H_{24}F_{12}O_2P_2Pt$	41.52	41.69	2.62	2.70	6.69	7.71
3	$Pd(L^1)_2$	$C_{32}H_{24}F_{12}O_2P_2Pd$	45.92	46.99	2.90	3.05	7.40	7.34
4	$Ni(L^1)_2$	$C_{32}H_{24}F_{12}NiO_2P_2$	48.70	48.61	3.07	3.08	7.85	7.99
5	$Co(L^1)_2$	$C_{32}H_{24}CoF_{12}O_2P_2$	48.68	48.61	3.06	3.28	7.85	7.58
6	$Cu(Ph_3P)_2(L^1)$	$C_{52}H_{42}CuF_6OP_3$	65.51	65.53	4.44	4.70	9.75	9.98
7	$Cu(L^2)_2$	$C_{32}H_{24}CuF_{12}O_4P_2$	46.36	46.53	3.01	2.93	7.01	7.50
8	$K[RhCl_2(L^1)_2]$	$C_{32}H_{24}Cl_2F_{12}KO_2P_2Rh$	40.74	40.96	2.56	2.58	6.57	5.76

Table II. Summary of Crystal and Data Collection Parameters

mol formula	$C_{32}H_{24}F_{12}NiO_2P_2$
fw	789.18
cryst class	orthorhombic
a	18.145 (2) Å
b	33.269 (3) Å
c	10.945 (1) Å
V	6607 (2) Å^3
Z	8
d(obsd)[a]	1.59 (1) g cm^{-3}
d(calcd)	1.587 g cm^{-3}
syst absences	$h00$, $h \neq 2n$
	$0k0$, $k \neq 2n$
	$00l$, $l \neq 2n$
space group	$P2_12_12_1$
diffractometer	Enraf-Nonius CAD4F
temp	22 °C
radiation	Cu Kα, λ = 1.541 85 Å
filter	Ni prefilter, 0.015 mm
aperture	4 mm × (4 + 0.15 tan θ) mm
exposure time	152 h
data collcd	$0 \leq h \leq 22$, $0 \leq k \leq 40$, $0 \leq l \leq 13$
θ range	$0.50° \leq 2\theta \leq 70°$
scan type	$\omega/2\theta$, at 0.9–4.0° min^{-1}
scan width	(0.65 + 0.15 tan θ)°
bkgds	25% above and below calcd scan width
std reflcns	6,0,0; 0,12,0; 0,0,2
loss in intens	0.01% h^{-1}, 1.6% overall
cryst dimens	0.41 × 0.53 × 0.42 mm
cryst v	0.029 60 mm^3
μ (Cu Kα)	26.67 cm^{-1}
abs cor	Gaussian, 10 × 8 × 8 grid
range trans coeff	0.457–0.580
cryst faces	{010}, {121}
	(222), ($\bar{2}\bar{2}2$), ($\bar{2}2\bar{2}$), ($\bar{2}\bar{2}\bar{2}$), ($2\bar{2}2$), ($\bar{2}22$)
	($\bar{2}\bar{2}0$), ($\bar{2}20$), ($\bar{1}\bar{2}0$), ($\bar{1}20$)
no. of reflcns collcd	6942
no. of data in final cycle	5922
σ	$I_o > 3\sigma(I_o)$
no. of variables, final cycle	407
final R_1[b]	0.0716
final weighted R_2[c]	0.0720

[a] By neutral buoyancy in cyclohexane/$C_2H_4Br_2$. [b] $R_1 = \sum||F_o| - |F_c||/\sum|F_o|$. [c] $R_2 = [\sum w(|F_o| - |F_c|)^2/\sum wF_o^2]^{1/2}$.

phenylphosphinomethyl)-1,1,1,3,3,3-hexafluoro-2-propanol, $Ph_2PCH_2C(CF_3)_2OH$ (HL^1, **1**), as a waxy solid (mp 59–62 °C) in 52% yield. Mass spectrum: parent ion m/e 366.

Complex Synthesis. Platinum(II) Complex, $Pt(L^1)_2$ (2). K_2PtCl_4 (1 g, 2.4 mmol) was dissolved in dimethylformamide (100 mL), and HL^1 (2 g, 5.5 mmol) in ethanol (20 mL) was added with stirring, followed by dropwise addition of ethanolic KOH (4.8 mmol. In this and subsequent reactions it was found convenient to measure out KOH as a standardized solution, ~0.3 M, in ethanol). The mixture was centrifuged to remove KCl, then stirred for 24 h at 25 °C, and centrifuged again, and DMF was removed by vacuum evaporation, leaving an oil. Addition of $CHCl_3$ precipitated white $Pt(L^1)_2$ (**2**): mp 289 °C; m/e 925.

Palladium(II) Complex, $Pd(L^1)_2$ (3). $PdCl_2(PhCN)_2$ 1 g, 2.6 mmol) was dissolved in $CHCl_3$ (50 mL), and HL^1 (2.1 g, 5.6 mmol) in ethanol (20 mL) was added, followed by dropwise KOH (5.2 mmol) in ethanol. Workup as before gave white $Pd(L^1)_2$ (**3**): mp 240–241 °C; m/e 836.

Nickel(II) Complex (4). $NiCl_2 \cdot 6H_2O$ (0.59 g, 2.5 mmol) was dissolved in ethanol (20 mL), and HL^1 (2 g, 5.5 mmol) in ethanol (20 mL) was added, causing the color to change from light green to yellow. On slow addition of ethanolic KOH (5.0 mmol), the color changed to orange. After the mixture was stirred for 24 h, KCl was removed by centrifugation and ethanol removed by rotary evaporation, leaving a yellow oil. Addition of ethanol gave green crystals of $Ni(L^1)_2$ (**4**): mp 330–331 °C; m/e 790. Visible spectra: see Discussion.

Cobalt(II) Complex (5). $CoCl_2 \cdot 6H_2O$ (0.33 g, 1.4 mmol) was dissolved in ethanol (100 mL), and HL^1 (1 g, 2.7 mmol) was added, followed by dropwise KOH (2.7 mmol); the color changed to orange. After removal of KCl and solvent, the resulting orange oil was extracted with CH_2Cl_2 and the product recrystallized from $CHCl_3/Et_2O$ to give orange $Co(L^1)_2$ (**5**): mp 283 °C; m/e 789; $\lambda_{max}(CH_2Cl_2)$ 405 nm (ϵ 177); λ_{max}(pyridine) 452 (76), 614 (26) nm.

Copper(I) Complex (6). $Cu(PPh_3)_3Cl$ (1 g, 1.1 mmol) was dissolved in $CHCl_3$, and HL^1 (0.5 g, 1.4 mmol) in ethanol was added, followed by ethanolic KOH (1.1 mmol). After the mixture was stirred for 24 h, solvent was removed, the residue extracted with CH_2Cl_2, KCl and solvent removed, and the product recrystallized from $CHCl_3/C_6H_{14}$ to give white $Cu(PPh_3)_2(L^1)$ (**6**): mp 166–168 °C; m/e 955.

Attempted Copper(II) Complex (7). When the procedure used for the Co^{2+} complex (**5**) was repeated with $CuCl_2$, extensive discoloration and precipitation was observed. Workup gave a blue crystalline product in low yield, but characterization by analysis and mass spectrum showed it to be the Cu^{2+} complex of the oxidized ligand, $Cu[P(=O)Ph_2CH_2C(CF_3)_2O]_2$, $Cu(L^2)_2$ (**7**): mp 252 °C; m/e 825, ν(P=O) 1082 cm^{-1}. No attempt was made to isolate the phosphine oxide ligand, HL^2.

Rhodium(III) Complex (8). $RhCl_3 \cdot 3H_2O$ (0.5 g, 1.9 mmol) was suspended in ethanol (20 mL), and HL^1 (2.1 g, 5.7 mmol) was added. The solid dissolved as ethanolic KOH (5.7 mmol) was slowly added, giving a yellow-orange solution. After the mixture was stirred for 24 h, solvent was removed and the residue extracted with CH_2Cl_2. Removal of KCl and solvent left a yellow oil, recrystallized from $CHCl_3/C_6H_{14}$ to give orange $K[RhCl_2(L^1)_2]$ (**8**): mp 291 °C; m/e 942; λ_{max} (acetone) 435 nm (ϵ 380).

Complexes were characterized by elemental analysis (Table I) and mass spectra. The latter showed a parent ion corresponding to the expected formulation in each case, including the potassium cation for the anionic rhodium complex **7**. All complexes showed infrared spectra consistent with their proposed structures, dominated by strong C–F absorptions in the region 1160–1190 cm^{-1}. NMR spectra are discussed later in this paper.

Structure Determination of $Ni(L^1)_2$ (4). Dark green crystals of compound **4** were obtained by slow evaporation of an acetone solution. A crystal was chosen for data collection having 20 faces, the longest dimension being approximately 0.53 mm.

(i) X-ray Data Collection and Reduction. Preliminary Weissenberg and precession photographs showed the space group to be $P2_12_12_1$ (D_2^4 No. 19),[13] and cell constants were determined. The crystal density, measured by flotation, indicated that there were two formula weights per equivalent position. The magnitude of b necessitated the use of Cu radiation for the collection of intensity data in order to minimize overlap of reflections. General conditions of data recording[14a] and processing[14b] are recorded in Table II.

Analysis of the intensity data for the standard reflections showed that no appreciable crystal decomposition occurred during data collection. The crystal faces were indexed by optical goniometry, and the dimensions were measured on a microscope fitted with a filar eyepiece. An absorption correction was carried out by Gaussian numerical methods using the program AGNOST.[15] A value of 0.04 was chosen for P.

(ii) Structure Solution and Refinement. The positions of the two Ni atoms were determined from a three-dimensional Patterson synthesis, which also suggested that the phosphorus atoms were in trans geometry about nickel. The peak heights in a difference-Fourier synthesis phased

(13) "International Tables for X-ray Crystallography"; Reidel: Dordrecht, The Netherlands 1983; Vol. A.
(14) (a) "Enraf-Nonius CAD4F Users' Manual"; Enraf-Nonius: Delft, The Netherlands 1984. (b) "Enraf-Nonius Structure Determination Package, SDP-Plus"; Enraf-Nonius: Delft, The Netherlands, 1982; Version 1.0.
(15) Cahen, D.; Ibers, J. A. *J. Appl. Crystallogr.* **1972**, *5*, 298.

Table III. Positional (×10⁴) and Thermal (×10³) Parameters for **4**

atom	x	y	z	U_{eq},[a] Å²	atom	x	y	z	U_{eq},[a] Å²
Ni(1)	1071.1 (7)	1267.8 (4)	306.6 (13)	36 (1)	C(16)	5697 (7)	881 (4)	7814 (11)	68 (3)
Ni(2)	5932.7 (7)	1236.3 (4)	4677.1 (13)	36 (1)	C(21)[b]	2892 (3)	1202 (2)	1264 (5)	40 (1)
P(1)	2202.2 (12)	1037.9 (7)	173 (2)	41 (1)	C(22)	2676 (3)	1225 (2)	2483 (6)	59 (1)
P(2)	−70.5 (11)	1473.0 (7)	393 (2)	43 (1)	C(23)	3180 (4)	1345 (2)	3370 (4)	72 (1)
P(3)	6015.8 (12)	1893.5 (6)	4674 (2)	39 (1)	C(24)	3899 (4)	1442 (2)	3039 (6)	71 (1)
P(4)	5866.9 (12)	575.7 (6)	4730 (2)	39 (1)	C(25)	4115 (3)	1418 (2)	1820 (7)	89 (1)
F(1)	1236 (4)	1701 (2)	−3631 (6)	111 (6)	C(26)	3611 (4)	1298 (2)	933 (5)	67 (1)
F(2)	1536 (5)	1094 (3)	−3417 (6)	120 (7)	C(31)	2260 (4)	499 (2)	108 (7)	49 (1)
F(3)	2383 (4)	1530 (3)	−3760 (6)	131 (7)	C(32)	1771 (4)	301 (3)	−665 (7)	96 (1)
F(4)	1492 (5)	2184 (2)	−1690 (8)	127 (7)	C(33)	1787 (4)	−117 (3)	−749 (7)	109 (1)
F(5)	2206 (4)	1973 (2)	−301 (7)	99 (5)	C(34)	2292 (6)	−336 (2)	−61 (9)	91 (1)
F(6)	2624 (5)	2068 (3)	−2066 (8)	148 (8)	C(35)	2781 (5)	−137 (3)	711 (8)	126 (1)
F(7)	32 (5)	538 (2)	1090 (8)	129 (7)	C(36)	2765 (4)	280 (3)	795 (6)	94 (1)
F(8)	−487 (5)	499 (3)	2841 (9)	155 (9)	C(41)	−177 (6)	2008 (1)	432 (6)	47 (1)
F(9)	656 (6)	376 (2)	2645 (10)	155 (9)	C(42)	−818 (3)	2200 (2)	50 (7)	75 (1)
F(10)	904 (5)	926 (3)	4286 (6)	141 (8)	C(43)	−875 (4)	2616 (2)	131 (8)	99 (1)
F(11)	539 (5)	1528 (3)	3949 (8)	150 (8)	C(44)	−291 (5)	2840 (1)	594 (8)	82 (1)
F(12)	−244 (5)	1077 (3)	4415 (6)	145 (8)	C(45)	350 (4)	2648 (2)	976 (7)	87 (1)
F(13)	6984 (4)	1216 (2)	913 (6)	101 (5)	C(46)	407 (3)	2232 (2)	895 (7)	78 (1)
F(14)	7056 (5)	1855 (2)	801 (6)	112 (6)	C(51)	−723 (3)	1298 (2)	−735 (6)	48 (1)
F(15)	6016 (4)	1572 (2)	1088 (6)	105 (3)	C(52)	−1359 (4)	1083 (2)	−450 (5)	68 (1)
F(16)	7696 (3)	1563 (2)	4310 (6)	92 (5)	C(53)	−1832 (3)	959 (2)	−1377 (7)	80 (1)
F(17)	8032 (3)	1836 (2)	2659 (7)	103 (6)	C(54)	−1671 (4)	1050 (2)	−2589 (6)	76 (1)
F(18)	7935 (3)	1203 (2)	2785 (7)	88 (5)	C(55)	−1036 (4)	1265 (2)	−2874 (5)	84 (1)
F(19)	4305 (4)	1301 (2)	7799 (7)	103 (5)	C(56)	−562 (3)	1389 (2)	−1947 (7)	71 (1)
F(20)	3940 (4)	1006 (2)	6225 (7)	108 (6)	C(61)	5173 (3)	2173 (2)	4636 (7)	44 (1)
F(21)	4128 (4)	672 (2)	7818 (8)	119 (6)	C(62)	4736 (4)	2152 (2)	5679 (5)	66 (1)
F(22)	5539 (5)	559 (3)	8511 (7)	133 (7)	C(63)	4066 (4)	2354 (2)	5720 (6)	90 (1)
F(23)	5677 (5)	1195 (2)	8516 (6)	117 (6)	C(64)	3832 (3)	2578 (2)	4717 (8)	87 (1)
F(24)	6382 (4)	833 (2)	7412 (7)	98 (5)	C(65)	4269 (4)	2599 (2)	3674 (6)	88 (1)
O(1)	1171 (4)	1421 (2)	−1299 (6)	56 (2)	C(66)	4940 (4)	2396 (2)	3633 (5)	72 (1)
O(2)	977 (4)	1126 (2)	1929 (6)	58 (2)	C(71)	6540 (3)	2123 (2)	5871 (5)	48 (1)
O(3)	6450 (3)	1240 (2)	3234 (6)	50 (2)	C(72)	6904 (4)	1880 (1)	6714 (7)	56 (1)
O(4)	5360 (4)	1245 (2)	6063 (6)	57 (2)	C(73)	7311 (4)	2054 (2)	7653 (6)	86 (1)
C(1)	2452 (5)	1211 (3)	−1354 (9)	54 (3)	C(74)	7356 (4)	2470 (2)	7749 (6)	85 (1)
C(2)	1847 (5)	1507 (3)	−1782 (9)	46 (2)	C(75)	6992 (5)	2713 (2)	6906 (8)	96 (1)
C(3)	−339 (6)	1304 (3)	1940 (10)	60 (3)	C(76)	6585 (4)	2539 (2)	5967 (6)	71 (1)
C(4)	304 (5)	1050 (3)	2453 (9)	45 (2)	C(81)	6708 (3)	306 (2)	5102 (7)	42 (1)
C(5)	6503 (5)	1985 (3)	3235 (9)	52 (2)	C(82)	6749 (4)	−2 (2)	5962 (6)	85 (1)
C(6)	6814 (5)	1576 (3)	2778 (8)	45 (2)	C(83)	7414 (5)	−199 (2)	6165 (7)	103 (1)
C(7)	5207 (5)	516 (3)	5968 (8)	46 (2)	C(84)	8039 (4)	−89 (3)	5507 (8)	82 (1)
C(8)	5176 (5)	902 (3)	6690 (8)	43 (2)	C(85)	7998 (3)	219 (3)	4647 (8)	110 (1)
C(9)	1757 (7)	1472 (4)	−3180 (12)	73 (3)	C(86)	7333 (4)	416 (2)	4444 (6)	84 (1)
C(10)	2051 (7)	1942 (4)	−1504 (12)	75 (3)	C(91)	5482 (4)	323 (2)	3418 (6)	47 (1)
C(11)	126 (9)	606 (4)	2302 (15)	92 (4)	C(92)	5398 (4)	−93 (2)	3396 (7)	81 (1)
C(12)	375 (9)	1175 (5)	3808 (14)	93 (4)	C(93)	5064 (5)	−278 (2)	2398 (8)	93 (1)
C(13)	6724 (6)	1550 (4)	1380 (11)	63 (3)	C(94)	4815 (4)	−47 (3)	1422 (7)	85 (1)
C(14)	7623 (6)	1551 (4)	3077 (11)	65 (3)	C(95)	4899 (4)	369 (2)	1444 (6)	93 (1)
C(15)	4395 (6)	972 (3)	7162 (10)	60 (3)	C(96)	5233 (4)	554 (2)	2442 (7)	75 (1)

[a] U_{eq} parameters are given by $U_{eq} = {}^1/_3\sum_i\sum_j U_{ij}a_i^*a_j^*\mathbf{a}_i\cdot\mathbf{a}_j$, where $U_{ij} = \beta ij/(2\pi^2 a_i^* a_j^*)$ Å², and the thermal ellipsoid is defined as $\exp[-(\beta_{11}h^2 + \beta_{22}k^2 + \beta_{33}l^2 + 2\beta_{12}hk + 2\beta_{13}hl + 2\beta_{23}kl)]$. [b] Positional parameters for C(21)–C(96) are derived parameters; group parameters are presented in Table S-IV and defined in ref 20.

by the nickel atoms confirmed this, but when the phosphorus atoms were included and refined, the resulting geometry was unsatisfactory in several respects. It soon became apparent that the relationship between the nickel atom coordinates (0.11, 0.13, 0.03 and 0.59, 0.12, 0.47) was leading to pseudosymmetry, a condition that was only broken by trial and error. Peaks could readily be identified on the Patterson map as nickel to donor atom vectors, but since we were unsure as to the coordination geometry, there were 32 different dispositions of P and O atoms possible. This number was reduced to 16 by assuming that the intrachelate angle at nickel was less than 90°, and a least-squares refinement and difference-Fourier synthesis were performed on a PDP 11/23+ computer, using the Enraf-Nonius structure determination package[14b] for each arrangement. Only one gave an acceptable geometry for the two NiO_2P_2 fragments and in due course led to the location of the remaining 92 non-hydrogen atoms. The refinement procedure used full-matrix least-squares refinement on F,[16] minimizing the function $\sum w(|F_o| - |F_c|)^2$, where the weighting factor $w = 4F_o^2/\sigma^2(F_o^2)$. Atomic scattering factors were taken from Cromer and Waber,[17] while those for hydrogen were from Stewart, Davidson, and Simpson.[18] Anomalous dispersion factors were included for Ni, P, O, and F atoms according to Cromer and Liberman.[19] Phenyl rings were refined as idealized rigid groups (C–C = 1.392 Å)[20] assigned group thermal parameters. With anisotropic thermal parameters, refinement coverged at $R_1 = 0.076$ and $R_2 = 0.080$. All 48 hydrogen atoms were located at electron densities ranging from 0.12 (9) to 0.56 (9) e Å⁻³. Subsequent cycles of least-squares refinement included the contributions from the hydrogen atoms with idealized geometry assumed, and R_1 and R_2 were reduced to 0.0716 and 0.0720. Limitations on computer storage[16] precluded the inclusion of individual isotropic thermal parameters for the group carbon atoms. However, by fixing the Ni and P atoms, sufficient storage could be made available for a determination of the relative magnitudes of the individual thermal parameters on each ring, and these corrections were applied to the overall group

(16) Computer programs used include local modifications of the following for the CDC Cyber 835 at the University of Western Ontario: WOCLS, full-matrix least-square refinement, from J. A. Ibers' NUCLS; Patterson and Fourier syntheses, FORDAP, by A. Zalkin; ORFFE, functions and errors, by W. R. Busing and H. A. Levy; ORTEPII, crystal structure illustrations, by C. K. Johnson.

(17) Cromer, D. T.; Waber, J. T. *Acta Crystallogr.* **1965**, *18*, 104.
(18) Stewart, R. F.; Davidson, E. R.; Simpson, W. T. *J. Chem. Phys.* **1965**, *42*, 3175.
(19) Cromer, D. T.; Liberman, J. *J. Chem. Phys.* **1970**, *53*, 1891.
(20) Eisenberg, R.; Ibers, J. A. *Inorg. Chem.* **1965**, *4*, 773.

Table IV. Selected Intramolecular Dimensions

molecule 1		molecule 2	
	Bond Lengths,[a] Å		
Ni(1)–P(1)	2.195 (2)	Ni(2)–P(3)	2.192 (2)
Ni(1)–P(2)	2.183 (2)	Ni(2)–P(4)	2.202 (2)
Ni(1)–O(2)	1.838 (7)	Ni(2)–O(3)	1.839 (7)
Ni(1)–O(2)	1.844 (7)	Ni(2)–O(4)	1.837 (6)
P(1)–C(1)	1.82 (1)	P(3)–C(5)	1.83 (1)
P(1)–C(21)	1.813 (6)	P(3)–C(61)	1.789 (7)
P(1)–C(31)	1.797 (7)	P(3)–C(71)	1.790 (7)
P(2)–C(3)	1.85 (1)	P(4)–C(7)	1.818 (9)
P(2)–C(41)	1.789 (7)	P(4)–C(81)	1.817 (7)
P(2)–C(51)	1.807 (7)	P(4)–C(91)	1.805 (7)
O(1)–C(2)	1.37 (1)	O(3)–C(6)	1.39 (1)
O(2)–C(4)	1.37 (1)	O(4)–C(8)	1.37 (1)
C(1)–C(2)	1.55 (1)	C(5)–C(6)	1.56 (1)
C(3)–C(4)	1.55 (1)	C(7)–C(8)	1.51 (1)
C(2)–C(9)	1.54 (1)	C(6)–C(13)	1.54 (1)
C(2)–C(10)	1.52 (1)	C(6)–C(14)	1.51 (1)
C(4)–C(11)	1.52 (1)	C(8)–C(15)	1.53 (1)
C(4)–C(12)	1.55 (1)	C(8)–C(16)	1.55 (1)
	Bond Angles,[b] deg		
P(1)–Ni(1)–O(1)	86.6 (2)	P(3)–Ni(2)–O(3)	87.5 (4)
P(2)–Ni(1)–O(2)	87.1 (2)	P(4)–Ni(2)–O(4)	87.9 (2)
Ni(1)–P(1)–C(1)	100.5 (3)	Ni(2)–P(3)–C(5)	101.6 (3)
Ni(1)–P(2)–C(3)	101.2 (3)	Ni(2)–P(4)–C(7)	99.4 (3)
Ni(1)–O(1)–C(2)	121.1 (6)	Ni(2)–O(3)–C(6)	123.9 (6)
Ni(1)–O(2)–C(4)	122.1 (6)	Ni(2)–O(4)–C(8)	122.4 (6)
C(1)–C(2)–O(1)	112.6 (8)	C(5)–C(6)–O(3)	114.5 (8)
C(3)–C(4)–O(2)	114.7 (8)	C(7)–C(8)–O(4)	115.9 (8)
P(1)–C(1)–C(2)	107.6 (7)	P(3)–C(5)–C(6)	107.8 (6)
P(2)–C(3)–C(4)	107.4 (7)	P(4)–C(7)–C(8)	108.8 (6)

[a] C–F bond lengths were in the range of 1.22 (1)–1.37 (1) Å. [b] C–C–F bond angles were in the range 105 (1)–116 (1)°; the F–C–F range was 103 (1)–112 (1)°.

parameters in subsequent refinements.

Since $P2_12_12_1$ is an acentric space group, the model was inverted to test for handedness, but this resulted in increases in R_1 and R_2 and the original model was therefore retained. The final cycle incorporated 40 variables with Ni, P, and F atoms assigned anisotropic thermal parameters and a single group thermal parameter for each phenyl group. The largest shift in the final cycle was 0.272 esd for the positional parameter of one phenyl group. The error on an observation of unit weight was 5.7 electrons, and a statistical survey of the 5922 data showed a satisfactory weighting scheme and no evidence for secondary extinction. Final atomic positions and U_{equiv} of non-hydrogen atoms for compound **4** are given in Table III, selected bond lengths and angles in Table IV, anisotropic temperature factors in supplementary Table S-I, hydrogen atom positions and temperature factors in Table S-II, least-squares planes in Table S-III, rigid group parameters in Table S-IV, and values of $10|F_o|$ and $10|F|$ in Table S-V.

Structure Description

Compound **4** crystallizes with two molecules per equivalent position in the unit cell. Both have the hybrid ligands arranged in trans square-planar geometry about nickel, but there are significant differences in the conformations of the chelate rings. ORTEP diagrams of the two molecules are shown as Figures 1 and 2, and the corresponding molecular dimensions are referred to as molecules 1 and 2, respectively, in the tables.

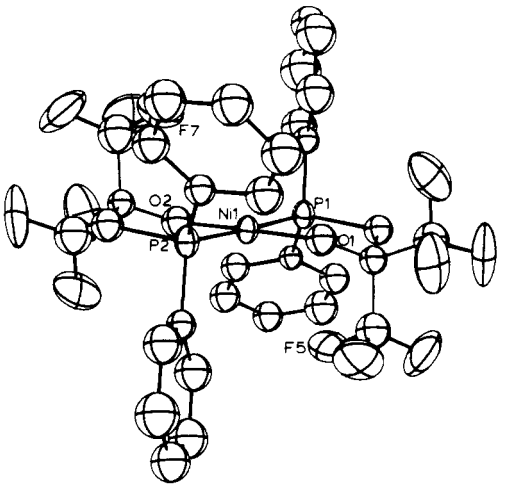

Figure 1. ORTEP diagram of $Ni[(C_6H_5)_2PCH_2C(CF_3)_2O]_2$ (**4**), molecule 1.

The following line diagrams show the atom numbering scheme used in each molecule:

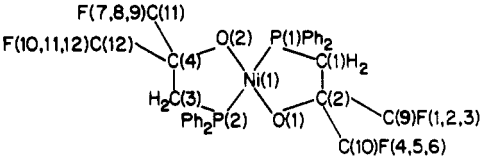

molecule 1. phenyl atoms C(21-26) and C(31-36) are attached to P(1)
phenyl atoms C(41-46) and C(51-56) are attached to P(2)

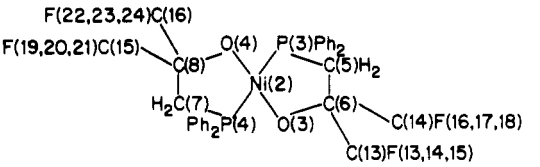

molecule 2. phenyl atoms C(61-66) and C(71-76) are attached to P(3)
phenyl atoms C(81-86) and C(91-96) are attached to P(4)

The color change from the orange solution to the green solid upon crystallization caused us to make a careful search for inter- and intramolecular interactions in the solid state. The crystals are built up from independent molecules, with no unusual intermolecular nonbonded contacts. The shortest F--H distances are 2.54 Å, between F(18) and H2C(3) at $(1 + x, y, z)$ and 2.59 Å between F(12) and HC(55) at $(x, y, 1 + z)$. A similar approach of 2.57 Å occurs between F(18) and HC(86) on different ligands in molecule 2. Similarly, there are no close approaches between H atoms in different molecules, the nearest being 2.52 Å between HC(86) and HC(83) at $(^3/_2 - x, -y, z - ^1/_2)$. The shortest F--F distances of approach are 2.82 Å between F(2) and F(10) at $(x, y, z - 1)$, and 2.99 Å between F(1) and F(11) at $(x, y, z - 1)$, rather shorter than twice the van der Waals radius for fluorine.

Table V. NMR Data[a]

			^1H (CH_2)		^{19}F (CF_3)		^{31}P	
no.	compd	solvent[b]	δ	$\lvert^2J(P,H)\rvert$[c]	δ	$^4J(P,F)$	δ	$\Delta\delta$[d]
1	$H(L^1)$	C	2.83 (d)		−77.4 (d)	16.5	−33.6	
2	$Pt(L^1)_2$	A	3.33 (d)[e]	12	−76.3 (s)[f]		17.3[g]	50.9
3	$Pd(L^1)_2$	A	3.47 (d)	12.5	−76.6 (d)	3.7	40.6	74.2
4	*trans*-$Ni(L^1)_2$	A	2.90 (t)	5.7[h]	−76.5 (t)	1.6[h]	14.5	48.1
4	*cis*-$Ni(L^1)_2$	A	3.26 (t)	6.5[h]	−76.7 (t)	2.6[h]	34.7	68.3
6	$Cu(PPh_3)_2(L^1)$	C	2.85 (d)	9.5	−77.8 (d)	6.8	−20.7[i]	12.9
8	$K[Rh(L^1)_2Cl_2]$	A	3.80 (d)	13	−77.4 (s)		32.0[j]	65.6

[a] At ambient temperature. J values in Hz. [b] C = $CDCl_3$; A = $(CD_3)_2CO$. [c] The sign of ^2J is probably negative; see text. [d] Coordination shift, $\Delta\delta = \delta_{coord} - \delta_{free}$. [e] $^3J(Pt,H) = 12$ Hz. [f] $^4J(Pt,F) = 11$ Hz. [g] $^1J(Pt,P) = 3517$ Hz. [h] Apparent coupling constants, see text. [i] PPh_3 signal at −4.2 ppm (singlet). [j] Doublet, $^1J(Rh,P) = 115$ Hz.

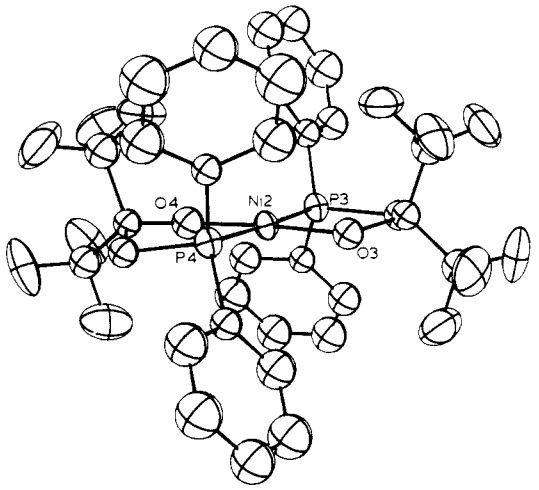

Figure 2. ORTEP diagram of $Ni[(C_6H_5)_2PCH_2C(CF_3)_2O]_2$ (**4**), molecule 2.

Although the two molecules have different conformations of the chelate rings, there is good agreement between chemically equivalent dimensions. Application of the χ^2 test showed that the four Ni–O bond lengths could be averaged to a value of 1.839 (2) Å. This is shorter than the normal range of 1.85–1.93 Å found in square-planar nickel(II) complexes,[21] or the value of 1.852 (3) Å in the anionic perfluoropinacolato complex $[Ni(PFP)_2]^{2-}$,[22] but it is comparable to the value of 1.842 (2) Å we have found in a neutral trans complex of nickel(II) with the N_2O_2 donor set.[23]

The C–O bonds in the chelating ligands could be averaged to 1.375 (5) Å. This is comparable to previously reported values of 1.380 (5)[22] and 1.362 (4) Å[23] for C–O bonds in chelated fluorinated alkoxides of nickel(II) and is in line with the trend on which we have previously commented[24] that the C–O bond in η^1-alkoxides of metals is significantly shortened.

The four Ni–P bond lengths could be averaged to give a value of 2.193 (3) Å. This is significantly shorter than the values usual for *trans*-$NiX_2(PR_3)_2$ complexes, which are in the range 2.25–2.30 Å.[25] A shorter Ni–P bond length of 2.175 (4) Å has been reported for *trans*-$Ni(C{\equiv}CPh)_2(PEt_3)_2$, and this is attributed to a strengthening of Ni–P π-bonding resulting from the transfer of electron density to the metal atom from the alkynyl ligands.[26] In the present compound, such an effect is unlikely because of the highly electronegative nature of the fluorinated alkoxide, and it seems more likely that the short Ni–P bond is the result of stronger σ-donation from phosphorus associated with electron withdrawal from the metal atom into the two alkoxide ligands. A further contributing factor in our systems may be the incorporation of the phosphine functions into chelate rings, and it may be significant that short trans Ni–P bonds [2.1975 (5) and 2.2086 (6) Å] are found when a multidentate ligand is used in the complex $NiCl[N(SiMe_2CH_2PPh_2)_2]$.[27]

In both forms of compound **4**, there is negligible departure from planar coordination at the metal, the average deviation from the least-squares planes of the NiP_2O_2 atoms being 0.031 and 0.037 Å for moleules 1 and 2, respectively (Table S-III). However, in molecule 1, the two carbon atoms in each chelate ring are on the same side of the coordination plane, with those bonded to oxygen, C(2) and C(4), farthest out of the plane. As a result, the CF_3 groups adopt strongly differentiated axial–equatorial conformations. This causes an approach from opposite sides of the coordination plane of the two axial CF_3 groups toward nickel, such that the closest Ni--F distances are 3.190 (8) and 3.193 (7) Å to F(5) and F(7), respectively, with F(5)--F(7) = 175.1 (2)°. Other short approaches are HC(46) and HC(32) from opposite sides at 2.97 and 3.23 Å respectively, with HC(46)--HC(32) = 168°.

In molecule 2, the two carbon atoms in the chelate ring are on opposite sides of the coordination plane, giving the ring an asymmetric skew conformation. The CF_3 groups then show a much smaller difference in their positions relative to the coordination plane than in molecule 1, and there are no comparable Ni--F approaches from opposite sides of the plane. Instead, F(16), and F(24) approach from the same side, at distances of 3.404 (7) and 3.380 (8) Å, respectively, with F(16)--Ni(2)--F(24) = 90.3(2)°. As was seen in molecule 1, there are also two Ni--H nonbonded approaches, to HC(72) and HC(96), both at 3.03 Å, with HC(72)--Ni(2)--HC(96) = 168°. The major difference in the geometries of the coordination spheres around nickel is thus in the significantly closer approaches of F(5) and F(7) in molecule 1, and possible consequences of this interaction are taken up in the Discussion.

Discussion

Ligand Synthesis. Our previous work has demonstrated that this highly electrophilic ketone will react readily with organolithium reagents to produce fluorinated tertiary alcohols $RC(CF_3)_2OH$. The group R may be alkyl or aryl, giving a monofunctional fluorinated alcohol,[28] or it may contain another functional group, and we have utilized the reagents formed by the lithiation of thioethers to prepare hybrid ligands containing both the hard fluoroalkoxy and the soft thioether functions.[2] The work of Peterson[12] has shown that methyl groups in tertiary phosphines may be lithiated by reaction with alkyllithium reagents in the presence of strongly coordinating nitrogen bases. Although considerable use for the preparation of hybrid ligands has been made of P-lithiated phosphines,[29] less attention has been given to the potential of those containing lithiated methyl groups. The reaction of such an intermediate with hexafluoroacetone should lead to molecules combining a dialkylphosphino and a fluorinated alcohol function, and we therefore used this approach for ligand synthesis:

$$CH_3{-}PPh_2 \xrightarrow{n\text{-BuLi/TMED}} LiCH_2{-}PPh_2 \xrightarrow[(2)\ H_3O^+]{(1)\ (CF_3)_2C{=}O} Ph_2P{-}CH_2{-}C(CF_3)_2OH$$

HL^1 (**1**)

Reaction of the lithiated phosphine with hexafluoroacetone is rapid at −78 °C. The synthesis thus proceeds without interference from the reaction of the ketone with the trivalent phosphine, a process which is well-known to lead to reductive dimerization and the formation of cyclic phosphoranes.[30] The product HL^1 (**1**) is a waxy solid showing no tendency to oxidation in air. Its NMR spectrum (Table V) is consistent with the proposed structure and shows the presence of traces of a compound tentatively identified as the ligand oxide, $Ph_2P(=O)CH_2C(CF_3)_2OH$: ^1H NMR (CH_2) δ = 2.86, $|^2J(P,H)|$ = 11.8 Hz.

Complex Synthesis. Our general approach to the preparation of metal ion complexes of fluorinated alcohols has been to treat the metal chloride, or a chloro complex, in suitable solvent (usually ethanol) with the ligand alcohol, followed by potassium hydroxide to deprotonate the alcohol and simultaneously remove Cl^- as insoluble KCl. This procedure was successfully applied to the

(21) Fox, M. R.; Lingafelter, E. C.; Sacconi, L. *Acta Crystallogr.* **1964**, *17*, 1159.
(22) Barnhart, D. M.; Lingafelter, E. C. *Cryst. Struct. Commun.* **1982**, *11*, 733.
(23) Martin, J. W. L.; Payne, N. C.; Willis, C. J. *Inorg. Chem.* **1978**, *17*, 3478.
(24) Boerē, R. T.; Payne, N. C.; Willis, C. J., unpublished observations.
(25) (a) Stalick, J. K.; Ibers, J. A. *Inorg. Chem.* **1970**, *9*, 453. (b) Scatteron, V.; Turzo, A. *J. Inorg. Nucl. Chem.* **1958**, *8*, 447. (c) Watkin, D. J. *J. Chem. Soc., Dalton Trans.* **1976**, 1803. (d) McPhail, A. T.; Steele, J. C. M. *J. Chem. Soc. A* **1972**, 2680.
(26) Davies, G. R.; Mais, R. H. B.; Austen, P. G. *J. Chem. Soc.* **1967**, 1750.
(27) Fryzuk, M. D.; MacNeil, P. A.; Rettig, S. J.; Secco, A. S.; Trotter, J. *Organometallics* **1982**, *1*, 918.
(28) Chang, I. S.; Price, J. T.; Tomlinson, A. J.; Willis, C. J. *Can. J. Chem.* **1972**, *50*, 512 and references cited therein.
(29) Uriarte, R.; Mazener, T. J.; Tau, K. D.; Meek, D. W. *Inorg. Chem.* **1980**, *19*, 79.
(30) Ramirez, F.; Smith, C. P.; Pilot, J. F.; Gulati, A. S. *J. Org. Chem.* **1968**, *33*, 3787.

preparation of neutral bis complexes of ligand **1**, $M(L^1)_2$, where M = Pt^{2+} (**2**), Pd^{2+} (**3**) Ni^{2+} (**4**), or Co^{2+} (**5**). The interaction of the ligand with Cu^{2+} followed a different course, with rapid oxidation occurring to give the phosphine oxide, $P(=O)Ph_2CH_2C(CF_3)_2OH$, HL^2, characterized as its copper(II) complex, $Cu(L^2)_2$ (**7**). This result was not unexpected, as copper(II) is known to be capable of oxidizing tertiary phosphines to the corresponding oxides.[31]

Since phosphine complexes of copper(I) are well established, we prepared the compound $Cu(PPh_3)_2(L^1)$ (**7**) by reaction of HL^1 with $(PPh_3)_3CuCl$. An anionic rhodium(III) complex was made containing two chelating ligands and two Cl^- ions, $[RhCl_2(L^1)_2]^-$ (**8**).

NMR Spectra and Structure. (i) Pt^{2+} and Pd^{2+} Complexes. We used NMR spectra (Table V) to assign the mode of attachment of the ligands. In the square-planar $M(L^1)_2$ complexes **2–4**, the corresponding groups on the two ligands may be in cis or trans geometry. For the platinum complex **2**, the value of $^1J(Pt,P)$ is 3517 Hz. This is very close to the value of 3578 Hz found in the perfluoropinacolato complex $Pt(PPh_2Me)_2(PFP)$, where the two phosphines are unambiguously cis to each other and trans to the fluoroalkoxide ligands.[32] Extensive studies on halide complexes $PtX_2(PR_3)_2$ have also shown that $^1J(Pt,P)$ is in the range 3500–3600 Hz for cis geometry, but 2400–2500 Hz for trans.[33] This evidence conclusively shows cis geometry for $Pt(L^1)_2$. In a recent study of the hybrid ligand $PPh_2CH_2CH_2OCH_3$, Anderson and Kumar[5b] find ^2J = 3650 Hz in *cis*-$PtCl_2(PPh_2CH_2CH_2OCH_3)_2$, where only the phosphines are coordinated; this increases to 4220 Hz in the chelated complex *cis*-$[Pt(PPh_2CH_2CH_2OCH_3)_2]^{2+}$.

The geometry of the palladium analogue **3** cannot be established so easily, because of the absence of coupling to the metal. The coordination shift of the ^{31}P resonance is 74.2 ppm, comparable to that of $Pt(L^1)_2$ (+50.9 ppm). Such data must be interpreted with caution, because of the variation in ^{31}P chemical shifts associated with incorporation into rings of various sizes.[34] The diphosphine complex $PdCl_2(Ph_2PCH_2CH_2PPh_2)$ has a ^{31}P coordination shift of 75.8 ppm[35] and forms a close analogy with **3**. Since the nickel complex **4** (discussed below) shows a mixture of cis–trans isomers in solution, cis geometry would be expected for the palladium and platinum analogues. Taking this in conjunction with the NMR data on $Pd(L^1)_2$, we assign it as cis.

In the free ligand, the coupling from phosphorus to CF_3 groups, $^4J(P,F)$, is 16.5 Hz, but coupling to the methylene protons, $^2J(P,H)$, is not seen. In the metal complexes, $^4J(P,F)$ is reduced to 3.7 Hz in $Pd(L^1)_2$ and is not detected in $Pt(L^1)_2$. At the same time, $^2J(P,H)$ becomes 12.5 Hz in $Pd(L^1)_2$ and 12 Hz in $Pd(L^1)_2$. The same effects are seen in other metal complexes in this study.

These trends can be rationalized by assuming that coupling constants from ^{31}P to ^1H and ^{19}F in the complexes are opposite in sign, with $^2J(P,H)$ being negative and $^4J(P,F)$ positive. It has long been recognized that reversal of sign in P–C–H couplings may easily occur[36] and that small or zero values of ^2J may result from fortuitous cancellation of contributing terms of different sign.[37] Thus, $^2J(P,H)$ = 2.8 Hz in $(CH_3)_3P$, decreasing by ~10 Hz to values of −7 to −8 Hz in complexes $(CH_3)_3PM(CO)_5$ (M = Cr, Mo, W).[38] With the phosphine $CH_3P(CF_3)_2$, $^2J(P,H)$ decreases from +4.4 to −6.8 Hz and $^2J(P,F)$ decreases from 74.5 to 70.0 Hz on coordination to $Cr(CO)_5$.[38] Similarly, $^2J(P,H)$ = −0.5 Hz in $(CH_3CH_2)_3P$[37] and is undetected (<1.0 Hz) in $CH_3CH_2PPh_2$,[40] but in the complex $(CH_3CH_2PPh_2)Cr(CO)_5$, $|^2J|$ = 7.0 Hz,[39] and this coupling should almost certainly be negative in sign, to be consistent with the general trend that coupling constants to phosphorus decrease on oxidation or coordination.[36]

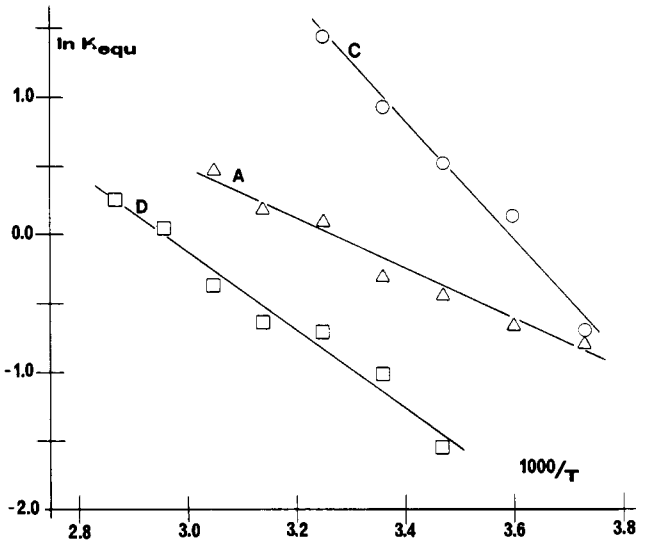

Figure 3. Plots of ln K_{eq} against $1000/T$: (A) acetone, (C) chloroform, (D) dichloromethane solution.

Table VI. Thermodynamic Data for Cis → Trans Conversion of **4**

solvent	dipole moment, D[a]	ΔH, kJ/mol	ΔS, J/mol	ΔG,[b] kJ/mol	K_{eq}[b]
$(CH_3)_2CO$	2.88	15.7	51.3	0.41	0.85
CH_2Cl_2	1.60	23.5	69.4	2.82	0.32
$CHCl_3$	1.01	35.5	127	−2.35	2.58
C_6H_6	0.0	*c*			

[a] "Lange's Handbook of Chemistry", 12th ed.; Dean, J. A., Ed.; McGraw-Hill: New York, 1972. [b] At 298 K. [c] Only trans isomer detected at all temperatures.

The value of $|^2J(P,H)|$ for the methylene protons in the free ligand $H(L^1)$ is 2.4 Hz, and by analogy with the similar phosphines discussed above, we assign it as positive. On coordination, this coupling decreases by 8–9 Hz in the Ni^{2+} complexes, giving negative values. The decrease is 12 Hz in the Cu^+ complex and 12–13 Hz in those of Pd^{2+}, Pt^{2+}, and Rh^{3+}. At the same time, the value of $^4J(P,F)$ decreases by ~10 Hz in the Cu^+ complex and by 13–17 Hz in the others. In the ligand oxide, the assignment of $^2J(P,H)$ as negative (−11.8 Hz) gives a decrease of 14.2 Hz on oxidation, consistent with previous reports.[36]

(ii) Ni^{2+} Complex. Solution Studies. The NMR spectra of $Ni(L^1)_2$ (**4**) indicate the presence of two species in a solvent and temperature-dependent equilibrium. In the ^{31}P NMR spectrum, two signals are seen in acetone solution at 14.5 and 34.7 ppm. Comparison of peak intensities in the ^{31}P, ^1H (CH_2), and ^{19}F NMR spectra at different temperatures shows that the upfield signal in each is associated with the species favored at higher temperature.

Two possibilities arise for isomerism in a nickel complex of this type: square-planar vs. tetrahedral geometry or cis–trans in square-planar geometry. The former, although known in phosphine complexes of nickel halides,[40] may be rejected on two grounds in the present case. First, the formation of a paramagnetic tetrahedral Ni^{2+} species would produce much more dramatic changes in the NMR parameters than those which we observe. Second, considerable changes in the visible absorption spectra would accompany such a change in ligand geometry, whereas we see no differences in the color of the solutions (orange) or the position of λ_{max}, which remains at 430 nm throughout. However, the intensity of the absorption decreases from $\epsilon \sim 1100$ for the low-temperature form to ϵ = 550 for the high-temperature form.

(31) Ondrejovic, G.; Makanova, D.; Valigura, D. *Z. Chem.* **1974**, *14*, 527.
(32) Boerē, R. T.; Willis, C. J. *Inorg. Chem.* **1985**, *24*, 1059.
(33) Grim, S. O.; Keiter, R. L.; McFarlane, W. *Inorg. Chem.* **1967**, *6*, 1133.
(34) Pregosin, P. S.; Kunz, R. W. *NMR: Basic Princ. Prog.* **1979**, *16*.
(35) Lindsay, C. H.; Benner, L. S.; Balch, A. L. *Inorg. Chem.* **1980**, *19*, 3503.
(36) Mavel, G. *Prog. Nucl. Magn. Reson. Spectrosc.* **1966**, *1*, 251 and references cited therein.
(37) Manatt, S. L.; Juvinall, G. L.; Elleman, D. D. *J. Am. Chem. Soc.* **1963**, *85*, 2664.
(38) Apel, J.; Bacher, R.; Grobe, J.; Le Van, D. *Z. Anorg. Allg. Chem.* **1979**, *453*, 39.
(39) Vincent, E.; Verdonck, L.; van der Kelen, G. P. *Spectrochim. Acta, Part A* **1980**, *36A*, 699.
(40) La Mar, G. N.; Sherman, E. O. *J. Am. Chem. Soc.* **1970**, *92*, 2691.

The visible spectra are consistent with the presence of two square-planar isomers with the same P_2O_2 donor set, the higher extinction coefficient being associated with the less symmetrical cis geometry, and this assignment is in agreement with the ^{31}P NMR data. The cis isomer, where the ^{31}P nuclei are trans to alkoxide, shows a coordination shift of 68.3 ppm, significantly greater than the value of 48.1 ppm found in the trans isomer.

This interpretation was confirmed by NMR studies in solvents of different polarity. Using acetone, dichloromethane, chloroform, and benzene, we ran ^{31}P NMR spectra over a range of temperatures, and values of K_{eq} for the cis–trans equilibrium were evaluated by integration in each case except benzene, where only the trans isomer could be detected. Plots of ln K_{eq} against $1/T$ were linear (Figure 3), and values of ΔG and ΔS, obtained from the slopes and intercepts, respectively, are given in Table VI.

Values of K_{eq} and ΔG give clear confirmation of the assignment of configurations. The nonpolar trans isomer is favored in benzene, but an increase in solvent polarity displaces the equilibrium toward the polar cis form. Since solvent interactions are at a minimum in benzene, we may conclude that this solution best approximates to the gaseous compound and that the trans form is, in isolation, the more stable isomer, with isomerization to the cis form occurring as a result of interactions with the more polar solvents.

Chatt and Wilkins[41] show that, for complexes $PtX_2(PR_3)_2$, metal–ligand bond strengths give the cis form a lower enthalpy content, and this is attributed to the mutually destabilizing effect of the two trans soft ligands, Pearson's "antisymbiotic effect".[42] However, this is of greater significance for soft ions, rather than for the relatively hard nickel(II) species, and it may be overwhelmed by the static contribution to ΔH, which would favor the trans isomer. The enthalpy of solution would favor the more polar cis isomer.

Contributions to ΔS for the isomerization come from steric effects and solvation. The former should be minimal, and the ΔS of solvation would favor the trans isomer, as the entropy of the solution would be reduced by the aggregation of solvent molecules around the more polar cis form.

Since variations in bond strengths and intramolecular steric effects between isomers are constant, the differences noted in Table IV must arise solely from solvation. As solvent polarity decreases, both ΔH and ΔS for the cis → trans conversion *increase*, and it is at first surprising that the ΔH contribution has the effect of stabilizing the polar cis form to the *greater* extent in the less polar solvent. We conclude that, while ΔH_{sol} decreases for both isomers as solvent polarity is reduced, the effect is greater for the nonpolar trans isomer. However, it is the change in ΔS that dominates as solvent polarity is reduced, leading to a greater proportion of the trans isomer in the less polar solvents.

There have been other reports of cis–trans isomerization in nickel(II) complexes.[43-46] For the isomerization of $NiBr_2(Cy_2PH)_2$ in CH_2Cl_2, ΔH = 23.6 kJ mol^{-1} and ΔS = 75.8 J mol^{-1},[46] while for the bis chelate Ni^{2+} complex of salicylaldoximine in the highly polar solvent Me_2SO (μ = 3.9 D), ΔH = 18.6 kJ mol^{-1} and ΔS = 45.6 J mol^{-1}.[45] These values compare closely with our results for CH_2Cl_2 and acetone solutions.

In the ^1H NMR spectrum of $Ni(L^1)_2$ at 25 °C, the ligand CH_2 signals for the cis and trans isomers appear at 3.26 and 2.90 ppm respectively. In each case, coupling to two ^{31}P nuclei would be expected, with a greater value for the directly bonded atom, $|^2J|$, than for the trans phosphine bonded through nickel, $|^4J|$.[47] However, our spectra show "virtual coupling", as if the phosphines were equivalent, to give a pseudotriplet peak for each isomer. Apparent coupling constants, interpreted on this basis, are 6.5 and 5.7 Hz for the cis and trans isomers, respectively. The ^{19}F signals in $Ni(L^1)_2$ show the same effect, with triplet patterns having apparent ^4J(P,F) values of 2.6 and 1.6 Hz for cis and trans isomers, respectively. In order to confirm that virtual coupling is observable in cis phosphine complexes of nickel(II), we have reexamined the spectra of the known perfluoropinacolato derivative $Ni(PFP)(PMePh_2)_2$,[48] which has the same donor set as **4** in cis geometry. Both ^1H and ^{13}C signals for the CH_3–P groups in the PFP^{2-} derivative are pseudotriplets, with apparent coupling constants of 5.5 and 13.6 Hz.

"Virtual coupling" represents a limiting case of situations where P–P′ coupling is much greater than coupling to other nuclei and is more common for trans complexes than cis. Palmer and Whitcomb,[46] using ^1J(P,H) values in Cy_2PH complexes of NiX_2, estimate coupling between equivalent ^{31}P nuclei as ~65 Hz for cis and ~380 Hz for trans isomers. Wada and Sameshima[49] have reported the NMR spectra of a variety of compounds $NiRR'(PR''_3)_2$, and find triplets for the CH_3–P signals in PMe_3 complexes with ^2J(P,H) values of 7–8 Hz; they suggest a trans configuration. While there is no reason to doubt this assignment, our results show that one cannot use the occurrence of a pseudotriplet signal in a Ni^{2+} complex as indicating trans geometry.

Because of the bidentate nature of the ligand, it seemed likely that the cis–trans interconversion of $Ni(L^1)_2$ was occurring intramolecularly via a tetrahedral transition state. The kinetics of the process may be followed by observing the methylene ^1H signals over a temperature range. Above 42 °C, a single peak is seen because of rapid isomer interconversion. This resolves into two broad singlets on cooling, and the triplet pattern of each of these becomes well resolved by 15 °C. The kinetics of the isomerization were studied by examining the effect on width at half-height, w^*, of the coalesced methylene proton signal that changing the concentration of complex and of introducing free ligand have. The rate of inversion was found to be first order in $[Ni(L^1)_2]$ and independent of $[HL^1]$, confirming an intramolecular process.

This is consistent with results of kinetic studies on the hybrid complex $Ni(MePhAs–PMePh)_2$, where the bidentate ligands were found to isomerize through an intramolecular process.[43] In platinum complexes, however, cis–trans isomerization occurs through the coordination of additional ligands.[50]

The value of w^* for the methylene peaks in $Ni(L^1)_2$ at the coalescence temperature of 42 °C in acetone is 33 Hz, and we have used this to determine the rate constants and $\Delta G^{\ddagger}$ values for the interconversion process.[51] The rate constants for the cis → trans and trans → cis reactions at 42 °C are 57 and 62 s^{-1} respectively, giving corresponding $\Delta G^{\ddagger}$ values of 66.7 ± 0.6 and 66.3 ± 0.5 kJ mol^{-1}. Although the isomerization may go through a tetrahedral intermediate, this barrier does not represent the difference in energy between square-planar and tetrahedral geometries. La Mar and Sherman[40] have shown that, in $NiX_2(R_3P)_2$ complexes where the two forms are very close in energy, $\Delta G^{\ddagger}$ for their interconversion is in the region 35–45 kJ mol^{-1} and the maximum in the reaction profile for cis ↔ trans conversion of $Ni(L^1)_2$ therefore lies at a configuration intermediate between square planar and tetrahedral.

(iii) Ni^{2+} Complex. Solid State. Both cis and trans isomers of $Ni(L^1)_2$ had the same orange color in solution, with λ_{max} = 430 nm. However, the crystals obtained from acetone solution were green, changing reversibly to orange on heating to 200 °C; cooling below 0 °C intensified the green color. A diffuse reflectance spectrum (25 °C) showed the 430-nm peak, with an additional absorption at 600 nm. By evaporation from ethanol, a metastable orange form of the complex was obtained; it slowly reverted to the green form at 25 °C, and a solid-state spectrum could not be obtained.

The green color of $Ni(L^1)_2$ must be associated with a specific solid-state interaction, either a tetrahedral distortion of the co-

(41) Chatt, J. J.; Wilkins, R. G. *J. Chem. Soc.* **1952**, 273, 4300.
(42) Pearson, R. G. *Inorg. Chem.* **1973**, *12*, 712.
(43) Salem, G.; Wild, S. B. *Inorg. Chem.* **1984**, *23*, 2655.
(44) Steltzer, O.; Unger, E. *J. Chem. Soc.* **1973**, 1783.
(45) Majer, J. R.; Al-Kuwarty, K. *Proc. Anal. Div. Chem. Soc.* **1978**, *15*, 98.
(46) Palmer, R. A.; Whitcomb, D. R. *J. Magn. Reson.* **1980**, *39*, 371.
(47) Absolute values of coupling constants are used in this discussion.
(48) Cripps, W. S.; Willis, C. J. *Can. J. Chem.* **1975**, *53*, 809.
(49) Wada, M.; Sameshima, K. *J. Chem. Soc., Dalton Trans.* **1981**, 240.
(50) Quagliano, J. V.; Schubert, L. *Chem. Rev.* **1952**, *50*, 220.
(51) Sandström, J. "Dynamic NMR Spectroscopy"; Academic Press: New York, 1982; p 77.

ordination plane or an increase in the coordination number of the metal through either intra- or intermolecular association. The interaction must be weak, since the solid is diamagnetic. In order to resolve this, and to determine whether cis or trans geometry is present in the solid, a structural determination was made.

It was found that the green form of $Ni(L^1)_2$ contains equal numbers of two types of molecule in the unit cell; these are shown as molecules 1 and 2 in Figures 1 and 2, respectively. In both molecules the geometry is trans, there is negligible departure from square-planar geometry at the metal atom, and the possibility that the green color is associated with a tetrahedral distortion may therefore be dismissed, neither is there any intermolecular association. However, in molecule 1 the ring conformations are such that fluorine atoms in the CF_3 groups on opposite sides of the coordination plane make an unusually close approach to the metal atom, and there are Ni--F distances of 3.190 (8) and 3.193 (7) Å. The F--Ni--F axis makes an angle of 55° with the coordination plane. The sum of the van der Waals radii for Ni and F is about 3.1–3.2 Å,[52] and we therefore suggest that this approach of the CF_3 groups represents weak additional coordination from fluorine to the metal. This interaction is responsible for the change in the absorption spectrum of the complex by distortion of the ligand field around the nickel(II) ion, without being sufficient to cause it to become paramagnetic.

Other features of the behavior of the complex may then be explained on this basis. The green color disappears in solution, or in the melt, because the specific conformation of the chelate rings in molecule 1 is only adopted in the solid state. Similarly, the intensity of the green color becomes less on raising the temperature of the solid because of a weakening of the Ni--F interaction. The metastable orange form of the solid probably contains the complex in a trans conformation similar to that of molecule 2, with no additional intramolecular interactions; this could then undergo a low-energy solid-state transformation into the green modification.

There are previous reports of diamagnetic, green nickel(II) complexes for which a weak axial interaction between the metal and additional ligands may be present, but complete structural information is generally lacking. For example, Hayter and Humiec have made an extensive investigation of complexes $NiX_2(PR_3)_2$, where X = Cl, Br, or I, and they were able to isolate both square-planar (diamagnetic) and tetrahedral (paramagnetic) forms in several cases.[53] However, for $NiI_2[P(i\text{-}C_3H_7)(C_6H_5)_2]_2$, they obtained a green, diamagnetic modification having properties incompatible with either conformation of ligands. Similarly, NiI_2 complexes with nitrogen donors such as quinoline,[54] lutidine,[55] tetramethylpyrazine,[56] or quinoxaline[57] give red or yellow colors in solution, changing to green in the solid state. The large, easily polarized I^- ion may be compared with a CF_3 group, and weak additional interactions between I^- and four-coordinate Ni^{2+}, similar to those we have demonstrated in $Ni(L^1)_2$, may be present.

(iv) Co^{2+} Complex (5). The orange color of **5** results from an absorption at 405 nm (ϵ = 177), strongly suggesting a square-planar rather than a tetrahedral arrangement, and the low value of the extinction coefficient[58] indicates trans geometry. This would be expected, on the basis of steric effects and the structure of the Ni^{2+} analogue. In pyridine solution, the color changed to green, probably as a result of solvation to a five-coordinate species.

(v) Cu^+ Complex (6). Since a Cu^{2+} complex was destabilized by the phosphine ligand, we used $CuCl(PPh_3)_3$ to prepare the stable complex $Cu(L^1)(PPh_3)_2$ (**6**). Its NMR spectrum shows a ^{31}P coordination shift of only 12.9 ppm, by far the smallest of all the complexes prepared in this study, and there is no coupling to ^{31}P in the PPh_3 coligands because of rapid exchange with free PPh_3; this effect has been observed in $Cu(PPh_3)_3Cl$.[59] The small value of the coordination shift, $\Delta\delta$, in this complex is consistent with that observed previously in complexes of monodentate phosphines; for example, $\Delta\delta$ for PEt_3 is 37.3 ppm in $PdCl_2(PEt_3)_2$[60] but only 4.8 ppm in $Cu(PPh_3)_3Cl$.[61]

(vi) Rh^{3+} Complex. The single ^{31}P NMR signal found in the anionic rhodium complex $K[RhCl_2(L^1)_2]$ (**8**) shows the two phosphines to be in equivalent environments, and the coupling to ^{103}Rh of 115 Hz demonstrates that they are trans to Cl^- or to $-C(CF_3)_3O^-$, rather than trans to each other. In complexes *mer*-$RhCl_3(PR_3)_3$, $^1J(Rh,P)$ is in the range 111–115 Hz for p trans to Cl^- but is in the range 83–83 Hz for p trans to PR_3.[62]

Conclusions

The results so far obtained in our study of this new hybrid ligand demonstrate its wide potential for the preparation of complexes of transition-metal ions of either hard or soft character. The strong bonding from the diphenylphosphino group to softer Lewis acids stabilizes their alkoxides and leads to a considerably extended chemistry of the important metal–oxygen bond. At the same time, the steric properties of the Ph_2P– group are very similar to those of other tertiary phosphines, enabling comparisons to be made with the considerable body of previous work on phosphine complexes.

Acknowledgment. We thank the Natural Sciences and Engineering Research Council of Canada for financial support of this work in the form of operating grants to N.C.P. and C.J.W. and postgraduate scholarships to R.T.B. and C.D.M.

Supplementary Material Available: Tables of temperature factors (Table S-I), hydrogen atom parameters (Table S-II), least-squares planes (Table S-III), rigid group parameters (Table S-IV), and $10|F_o|$ and $10|F_c|$ in electrons (Table S-V) (30 pages). Ordering information is given on any current masthead page.

(52) Bondi, A. *J. Phys. Chem.* **1964**, *68*, 441.
(53) Hayter, R. G.; Humiec, F. S. *Inorg. Chem.* **1965**, *4*, 1701.
(54) Goodgame, D. M. L.; Goodgame, M. *J. Chem. Soc.* **1963**, 207.
(55) Buffagni, S.; Vallarino, L. M.; Quagliano, J. V. *Inorg. Chem.* **1964**, *3*, 480.
(56) Lever, A. B. P.; Lewis, J.; Nyholm, R. S. *J. Chem. Soc.* **1963**, 5042.
(57) Lever, A. B. P. *J. Inorg. Nucl. Chem.* **1965**, *27*, 149.
(58) Nicolini, M.; Pecile, C.; Turco, A. *Coord. Chem. Rev.* **1966**, *1*, 133.
(59) Lippard, S. J.; Mayerle, J. J. *Inorg. Chem.* **1972**, *11*, 753.
(60) Mann, B. E.; Masters, C.; Shaw, B. L.; Slade, R. M.; Stainbank, R. E. *Inorg. Nucl. Chem. Lett.* **1975**, *7*, 881.
(61) Axtell, D. D.; Yoke, J. T. *Inorg. Chem.* **1973**, *12*, 1265.
(62) Mann, B. E.; Masters, C.; Shaw, B. L. *J. Chem. Soc., Dalton Trans.* **1972**, 704.